J. Plasma Physics (2012), vol. 78, part 1, pp. 39–45. © Cambridge University Press 2011
doi:10.1017/S0022377811000341

Optical guiding in a plasma channel having top-hat refractive index radial profile

F. SOHBATZADEH, S. MIRZANEJHAD and M. GHALANDARI

Department of Physics, Faculty of Science, University of Mazandaran, Babolsar, Iran
(f.sohbat@umz.ac.ir)

(Received 25 January 2011; revised 24 Febuary 2011 and accepted 8 July 2011; first published online 4 August 2011)

Abstract. In this paper, intense laser pulse guiding through a weakly ionized plasma channel is studied numerically. The radial profile of the channel refractive index is assumed to be top-hat. The propagating intense laser pulses are Gaussian TEM_{00} and Laguerre–Gaussian LG_{01} modes. The analysis includes the effects of plasma density inhomogeneity, diffraction, further ionization by the propagating laser pulse and nonlinearity arising from the nonlinear Kerr effect. Matched conditions are obtained for both TEM_{00} and LG_{01} laser modes for a top-hat refractive index profile. It is seen that the electron density profile changes the matched condition in the transmission of the laser pulse through the plasma channel. It is also shown that the nonlinear Kerr effect changes the matched condition and becomes the dominant effect in intense laser pulse propagation through the weakly ionized plasma channel.

1. Introduction

The guiding of intense laser pulses in plasmas is worth of attention for a wide range of applications, such as x-ray lasers, high harmonic generation and wakefield acceleration [1–6]. For all such applications, the interaction length is limited by diffraction to the order of the Rayleigh length. A waveguide can be used to guide the laser beam and increase the distance over which the peak laser intensity can be maintained. The physical processes underlaying this effect are now well understood. Optical guiding in a non-uniform plasma channel arises from a dynamic competition between refraction and diffraction of laser beam. Several methods of guiding, such as relativistic guiding [7, 8], Z-pinch waveguide [9], grazing incidence waveguide [10, 11], gas-filled capillary discharge [12, 13] and waveguide formed by hydrodynamic expansion [14–19] have been successfully examined. Measured electron density profiles of the capillary discharges as a function of delay time between the laser pulse injection and onset of the discharge current pulse indicate that the electron density profile changes during the time. This effect influences the matched condition and in turn the laser pulse energy transmission [12, 13]. The aim of this paper is to study the propagation of laser beam through a type of plasma waveguide that have the top-hat refractive index profile. In this plasma channel, the electron density differs from the parabolic channel that has been previously discussed experimentally and theoretically [12, 13, 20–23]. The top-hat plasma channel can be produced either by an intense Laguerre–Gaussian (LG_{01}) laser pulse or a capillary discharge at the early stages of plasma formation in a long capillary [12]. On the other hand, hydrodynamic expansion of a laser-produced plasma filament could yield this density profile in gases [24]. This plasma waveguide differs from the hollow plasma channel of Chiou et al. [25] that the channel is completely evacuated. For example, in the case of laser-produced plasma channel by a LG_{01} laser mode through multi-photon ionization of molecules of a gas such as oxygen or nitrogen, one can assume the electron density profile to be

$$n_e(r) = \Delta n_e \left(\frac{r^2}{r_{ch}^2}\right)^N e^{-N\left(\frac{r^2}{r_{ch}^2}\right)}, \qquad (1)$$

where r is the transverse coordinate, r_{ch} is the channel radius, $\Delta n_e = \Delta n_{e,ch} \times e^N$ is the channel characteristics and $\Delta n_{e,\,ch}$ is the channel depth or the maximum transverse electron density difference. Equation (1) specifies that N photons of the laser pulse are absorbed by gas molecules to form plasma [26]. For oxygen and nitrogen gases $N = 8$ and 11, respectively. In this channel, the refractive index at the axis is assumed to be $n_r = 1$ and that of the periphery of the channel $n_r = \sqrt{1 - \omega_p^2(r)/\omega^2}$, where $\omega_p = \sqrt{4\pi n_e(r)e^2/m}$ and ω is the laser wave angular frequency. The electron density profile and corresponding square of the top-hat refractive index profile are shown in Fig. 1. Therefore, the laser can be confined as if it were in an graded index optical fiber. Expressing the electron density profile of the plasma channel by (1), the coupled electromagnetic equations are derived for Gaussian TEM_{00} and LG_{01} laser pulse propagating in the proposed plasma channel. It is seen that the matched condition for the guided laser beam depends on the laser mode. The formulation includes the effects of plasma density inhomogeneity, diffraction, further ionization by the propagating laser pulse and nonlinearity arising from the nonlinear Kerr effect. The latter effect becomes the dominant process at high intensity regime and

https://doi.org/10.1017/S0022377811000341 Published online by Cambridge University Press

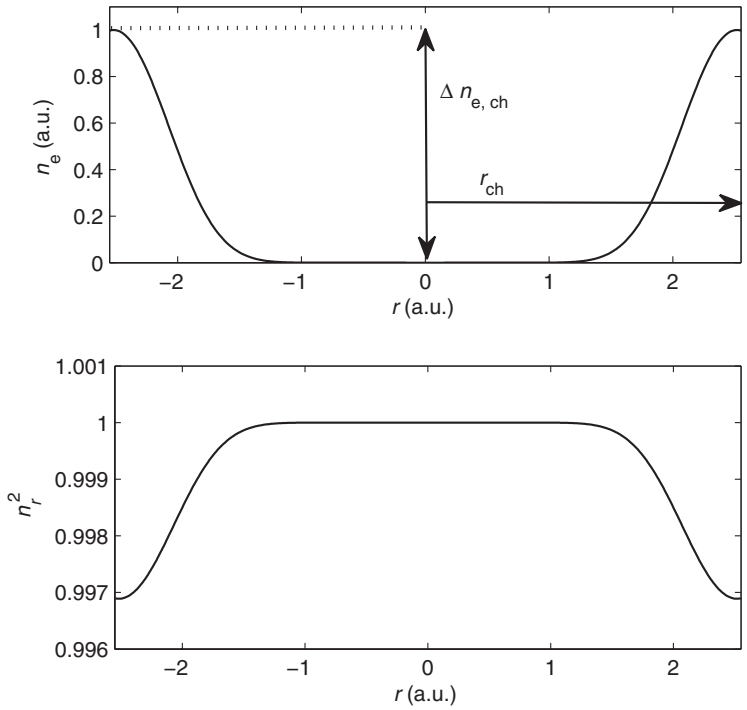


Figure 1. (a) Radial profile of electron density with channel depth $\Delta n_{e,ch}$ and channel radius r_{ch}, and (b) square of top-hat radial profile of the corresponding refraction index inside the channel.

drastically changes the matched condition of the propagating laser beam through the plasma channel.

The organization of this paper is as follows. The equations for the laser wave envelope and matched conditions are derived in Sec. 2. In Sec. 3, numerical results of the two laser modes propagating through the plasma channel are presented. Finally, in Sec. 4 the results and discussions are given.

2. Matched conditions for propagation of Gaussian TEM_{00} laser mode

A laser beam propagating through a plasma channel can be matched to guide with an approximate constant profile. Matched guiding means that the beam propagates through the channel with a constant spot size tailored to the parameters of the plasma channel. Assuming the plasma channel with top-hat refractive index profile, the matched condition for the TEM_{00} and LG_{01} laser beams propagating through the channel can be derived by starting from the wave equation for the laser electric field $\vec{E}(\vec{r},t)$ given by

$$\left(\nabla_\perp^2 + \frac{\partial^2}{\partial z^2} - \frac{1}{c^2}\frac{\partial^2}{\partial t^2}\right)\vec{E}(\vec{r},t) = \vec{S}(\vec{r},t), \qquad (2)$$

where, $\nabla_\perp^2$ denotes the transverse Laplasian operator in the cylindrical coordinate, c is the speed of light in vacuum and z-coordinate indicates the direction of propagation. The quantity $\vec{S}(\vec{r},t)$ represents the source term [23]. The laser electric field $\vec{E}(\vec{r},t)$ and the source term $\vec{S}(\vec{r},t)$ are written in terms of complex amplitudes $A(\vec{r},t)$ and $S(\vec{r},t)$, i.e.

$$\vec{E}(\vec{r},t) = \frac{1}{2}A(\vec{r},t)e^{i(kz-\omega t)}\hat{x} + \text{c.c.}, \qquad (3)$$

$$\vec{S}(\vec{r},t) = \frac{1}{2}S(\vec{r},t)e^{i(kz-\omega t)}\hat{x} + \text{c.c.}, \qquad (4)$$

where k is the carrier wave number, $\hat{x}$ is a unit vector in the direction of polarization and c.c. denotes the complex conjugate. Here, the source term includes inhomogeneous plasma density, the nonlinear Kerr self-focusing effect and the finite transverse effect of the laser beam, i.e.

$$S(\vec{r},t) = \left[\frac{\omega_p^2(\vec{r},\tau)}{c^2} - \frac{\omega^2 n_2}{4\pi c}|A|^2 - \frac{4}{r_{s0}^2}\right]A(\vec{r},t), \qquad (5)$$

where r_{s0} is the initial spot size of the laser pulse and n_2 is the nonlinear Kerr refractive index. Here, $\omega_p(\vec{r},\tau)$ contains both the plasma channel inhomogeneity and the extra ionization by the propagating laser pulse through the channel. In order to continue, we first consider the propagation of TEM_{00} laser pulse through the plasma channel. The electric field of the TEM_{00} laser mode can be given by

$$\vec{E}_{TEM_{00}}(\vec{r},t) = \frac{1}{2}\sqrt{\frac{16P_{in}}{cr_s^2(z,t)}}e^{-\frac{r^2}{r_s^2(z,t)}}e^{-\frac{ikr^2}{2R(z,t)}}e^{i(kz-\omega t)}$$

$$\times e^{-4\left(\frac{t-t_0}{\tau_p}\right)^2}\hat{x} + \text{c.c.}, \qquad (6)$$

where P_{in} is the input power, $r_s(z,t)$ is the spot size, $R(z,t)$ is the wave front curvature and t_p is the pulse duration. In order to obtain matched condition for the

https://doi.org/10.1017/S0022377811000341 Published online by Cambridge University Press

prescribed laser beam , we use the source- dependent expansion (SDE) method that was originally developed by Sprangle et al. [27]. In the SDE formulation, a reduced wave equation of the general form

$$\left(\nabla_{\perp}^2 + 2ik\frac{\partial}{\partial z}\right) A(\vec{r},\tau) = S(\vec{r},\tau) \tag{7}$$

is solved by the self-similar method. Here, τ and z are independent variables, where $\tau = t - z/v_g$ and v_g is the group velocity of the laser pulse. Concerning (6), one can use the trail solution for the complex electric field amplitude $A(\vec{r},\tau)$ as bellow:

$$A(r,z,\tau) = B(z,\tau)e^{i\Phi(z,\tau)}e^{-[1-i\alpha(z,\tau)]\frac{r^2}{r_s^2(z,\tau)}}, \tag{8}$$

where B is the field amplitude, Φ is the phase, and α is related to the curvature of the wave front. Quantities B, Φ, r_s, and α are real functions of z and τ that will be obtained for a matched beam propagating through the plasma channel. Using the SDE method, a set of self-consistent coupled equations for the pulse amplitude, phase, spot size and wave front curvature can be derived. Then, one can find the following equations governing the propagation of the TEM_{00} laser mode through the plasma channel as

$$\frac{\partial B}{\partial z} = -\frac{2\alpha B}{kr_s^2} + F_{\mathrm{I}} + G_{\mathrm{I}}, \tag{9}$$

$$\frac{\partial \Phi}{\partial z} = -\frac{2}{kr_s^2} - \frac{F_{\mathrm{R}}}{B} - \frac{G_{\mathrm{R}}}{B}, \tag{10}$$

$$\frac{\partial r_s}{\partial z} = \frac{2\alpha}{kr_s} - r_s\frac{G_{\mathrm{I}}}{B}, \tag{11}$$

$$\frac{\partial \alpha}{\partial z} = \frac{2(1+\alpha^2)}{kr_s^2} + 2\frac{G_{\mathrm{R}}}{B} - 2\alpha\frac{G_{\mathrm{I}}}{B}, \tag{12}$$

where the subscripts R, I denote the real and imaginary parts of each function, respectively. The complex functions F and G are given by

$$F = \frac{1}{2k}\int_0^{\infty} S(r,z,\tau)e^{-(1+i\alpha)\frac{r^2}{r_s^2}}e^{-i\Phi}\,d\left(2\frac{r^2}{r_s^2}\right), \tag{13}$$

$$G = \frac{1}{2k}\int_0^{\infty} S(r,z,\tau)\left(1-2\frac{r^2}{r_s^2}\right)e^{-(1+i\alpha)\frac{r^2}{r_s^2}}e^{-i\Phi}\,d\left(2\frac{r^2}{r_s^2}\right). \tag{14}$$

In the case of partially ionized plasma channel, the electron density profile of the channel can be changed by the powerful propagating laser pulse. This modification could be due to both further ionization and ponder-motive force of the propagating laser pulse. To take into account the ionization by the laser pulse, plasma angular frequency is described by $\omega_{\mathrm{p}}^2(r,z,\tau) = 4\pi e^2[n_{\mathrm{e}}(r) + n_{\mathrm{e}}'(r,z,\tau)]/m_{\mathrm{e}}$, where $n_{\mathrm{e}}(r)$ is given by (1) and

$$\frac{\partial n_e'(r,z,\tau)}{\partial \tau} = \frac{2\pi\omega}{(N-1)!}\left[\frac{I(r=0)}{I_{\mathrm{mp}}}\right]^N (n_{\mathrm{n}} - n_{\mathrm{e0}})e^{-2N(\frac{r}{r_s})^2} \tag{15}$$

is the rate equation for the produced electron density due to multiphoton ionization of the channel by the Gaussian laser pulse. $n_{\mathrm{e0}}(z,\tau)$ is the on-axis electron density. Here, I_{mp} is multiphoton ionization intensity, n_{n} is the neutral gas density, $I(r=0)$ is the laser intensity at r = 0. Substituting (5) into (13) and (14) gives

$$F(z,\tau) = -\frac{2}{kr_{s0}^2}B - \frac{\omega^2 n_2}{16k\pi c}|B|^2 B + \frac{2\pi e^2 n_{e0}}{mc\omega}B\left(\frac{1}{N+1}\right) + \frac{2\pi e^2 \Delta n_e B}{kmc^2}\left(\frac{r_s}{\sqrt{2}r_{\mathrm{ch}}}\right)^{2N}\left(\frac{N!}{\left(N\left(\frac{r_s}{\sqrt{2}r_{\mathrm{ch}}}\right)^2+1\right)^{(N+1)}}\right), \tag{16}$$

$$G(z,\tau) = -\frac{\omega^2 n_2}{32k\pi c}|B|^2 B + \frac{2\pi e^2 n_{\mathrm{e0}}}{mc\omega}B\left(\frac{N}{(N+1)^2}\right) + \frac{2\pi e^2 \Delta n_e B}{kmc^2}\left(\frac{r_s}{\sqrt{2}r_{\mathrm{ch}}}\right)^{2N}\left(\frac{N!}{\left(N\left(\frac{r_s}{\sqrt{2}r_{\mathrm{ch}}}\right)^2+1\right)^{(N+1)}} - \frac{(N+1)!}{\left(N\left(\frac{r_s}{\sqrt{2}r_{\mathrm{ch}}}\right)^2+1\right)^{N+2}}\right). \tag{17}$$

Finally, substituting (16) and (17) into (9)–(12), the equations governing the laser pulse amplitude $B(z,\tau)$, phase $\Phi(z,\tau)$, wavefront curvature $\alpha(z,\tau)$ and spot size $r_s(z,\tau)$ are found to be

$$\frac{\partial B}{\partial z} = -\frac{2\alpha B}{kr_s^2}, \tag{18}$$

$$\frac{\partial \Phi}{\partial z} = -\frac{2}{kr_s^2} + \frac{2}{kr_{s0}^2} + \frac{3\omega^2 n_2}{32k\pi c}|B|^2 - \frac{2\pi e^2 n_{e0}}{mc\omega}\left(\frac{2N+1}{(N+1)^2}\right) + \frac{2\pi e^2 \Delta n_e}{kmc^2}\left(\frac{r_s}{\sqrt{2}r_{\mathrm{ch}}}\right)^{2N} \times \left(\frac{-2\times N!\left(N\left(\frac{r_s}{\sqrt{2}r_{\mathrm{ch}}}\right)^2+1\right)+(N+1)!}{\left(N\left(\frac{r_s}{\sqrt{2}r_{\mathrm{ch}}}\right)^2+1\right)^{N+2}}\right), \tag{19}$$

https://doi.org/10.1017/S0022377811000341 Published online by Cambridge University Press

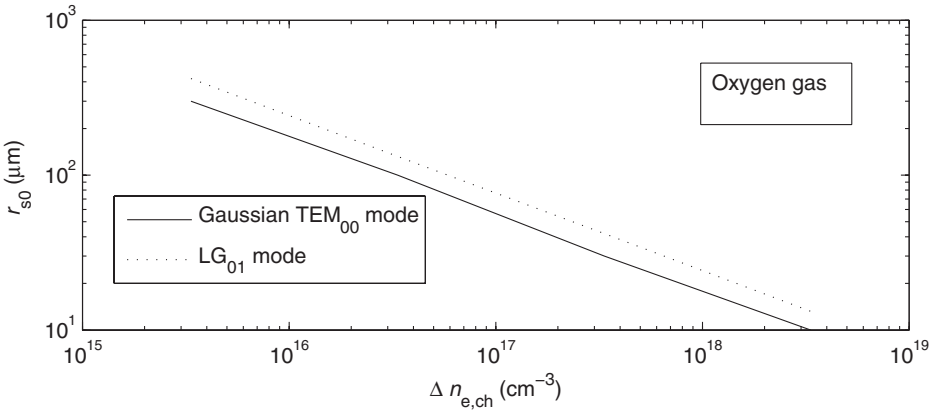


Figure 2. Variation of the matched spot size versus the channel depth in the optical guiding regime.

$$\frac{\partial\alpha}{\partial z}=\frac{2(1+\alpha^2)}{kr_s^2}-\frac{\omega^2 n_2}{16k\pi c}|B|^2+\frac{4\pi e^2 n_{e0}}{mc\omega}\left(\frac{N}{(N+1)^2}\right)+\frac{4\pi e^2\Delta n_e}{kmc^2}\left(\frac{r_s}{\sqrt{2}r_{\rm ch}}\right)^{2N}\times\left(\frac{N!\left(N\left(\frac{r_s}{\sqrt{2}r_{\rm ch}}\right)^2+1\right)-(N+1)!}{\left(N\left(\frac{r_s}{\sqrt{2}r_{\rm ch}}\right)^2+1\right)^{N+2}}\right),\quad(20)$$

$$\frac{\partial r_s}{\partial z}=\frac{2\alpha}{kr_s}.\quad(21)$$

In order to guide the laser pulse through the plasma channel, (18)–(21) must be set to zero. Equations (21) and (18) lead to $\alpha=0$ and B = cte., respectively. It means that the laser beam amplitude and wavefront curvature of the laser beam do not change during the propagation through the plasma channel. Finally, from (20) a matched condition for guiding the TEM_{00} mode through the plasma channel with the top-hat refractive index profile is obtained. The matched condition leads to the following equation:

$$NN!b_1x^{2N+2}(1-x^2)-(1-b_2|B|^2x^2+b_3n_{e0}x^2)(Nx^2+1)^{N+2}=0,\quad(22)$$

where $x=r_s/\sqrt{2}r_{\rm ch}$, $b_1=4\pi r_e\Delta n_e r_{\rm ch}^2$, $b_2=\omega^2n_2r_{\rm ch}^2/16\pi c$, $b_3=4\pi r_e r_{\rm ch}^2[N/(N+1)^2]$ and $r_e=e^2/mc^2$ is the classical electron radius. In (22), the term $b_2|B|^2$ indicates the self-focusing effect due to the nonlinear Kerr effect. Equation (22) has $2N+6$ roots for given values of b_1, $b_2|B|^2$ and b_3n_{e0}. Among the roots, only real and positive roots are acceptable for the matched guiding.

In order to investigate the matched condition for propagating LG_{01} mode through the top-hat plasma channel, an equation similar to (22) was obtained in the Appendix. One can obtain the following matched condition by taking into account plasma density inhomogeneity, nonlinear Kerr effect and finite size effect of the LG_{01} laser beam as

$$b_1x^{2N+2}(N+1)!\frac{N}{2}(1-2x^2)-(1-b_4|B|^2x^2+b_5n_{e0}e^Nx^2)(Nx^2+1)^{N+3}=0,\quad(23)$$

where $b_4=b_2/4$ and $b_5=2\pi r_e r_{\rm ch}^2N(N+1)!/(N+1)^{N+3}$.

3. Numerical results

In this section we present numerical results of solving (22) and (23) for TEM_{00} and LG_{01} laser modes with $\lambda=800$ nm and $\tau_p=100$ fs. It can be shown that the nonlinear Kerr effect is negligible when $I\leqslant\omega_p^2/2n_2\omega^2$. For example, assuming the channel depth to be $1.67\times10^{17}\,W/cm^2$, at intensities less than $1.2\times10^{14}\,\mathrm{W/cm^2}$, the nonlinear Kerr effect does not affect the optical guiding of the laser pulse. In our model, one can recall this region by the optical guiding regime. In this case the minimum channel radius has been obtained for the minimum channel depth in which the laser beam can be guided. The results can be formulated for oxygen gas plasma channel with TEM_{00} mode as given below:

$$r_{\rm ch}\simeq3.2\frac{c}{\omega_p},\quad r_{s0}\simeq0.98r_{\rm ch},\quad(24)$$

and for LG_{01} mode

$$r_{\rm ch}\simeq4.5\frac{c}{\omega_p},\quad r_{s0}\simeq0.72r_{\rm ch}.\quad(25)$$

In order to guide the laser modes through the top-hat plasma channel, there are sets of minimum channel depth $\Delta n_{\rm e,ch}$, channel radius $r_{\rm ch}$ and matched radius r_s. Higher the channel depth, lower laser spot size. This effect is depicted in Fig. 2. Equations (24) and (25) indicate the measure of required channel depth for a given channel radius to guide the aforementioned laser beams. The matched conditions for $I\geqslant\omega_p^2/2n_2\omega^2$ changes and self-focusing effect play the main role. It is found that the laser beam undergoes the nonlinear Kerr self-focusing during optical guiding through the plasma channel. This effect strongly depends on the laser intensity and channel depth. Figures 3 and 4 show

https://doi.org/10.1017/S0022377811000341 Published online by Cambridge University Press

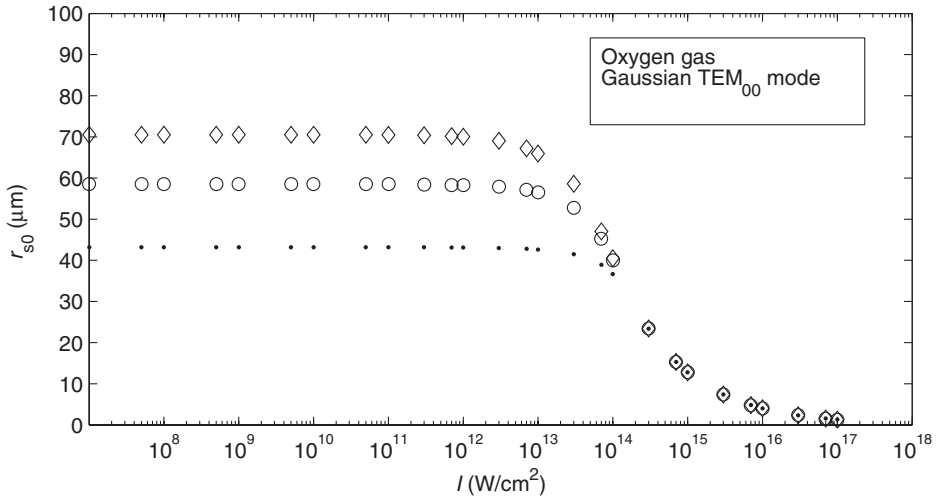


Figure 3. Variation of the matched initial spot sizes versus the intensity of the incident TEM_{00} laser pulse propagating through a top-hat plasma channel with radius of $r_{ch} = 100\ \mu$m. Dot (·) for $\Delta n_{e,ch} = 1.67 \times 10^{18}\ cm^{-3}$, circle (○) for $\Delta n_{e,ch} = 1.67 \times 10^{17}\ cm^{-3}$ and diamond (◇) for $\Delta n_{e,ch} = 6.67 \times 10^{16}\ cm^{-3}$.

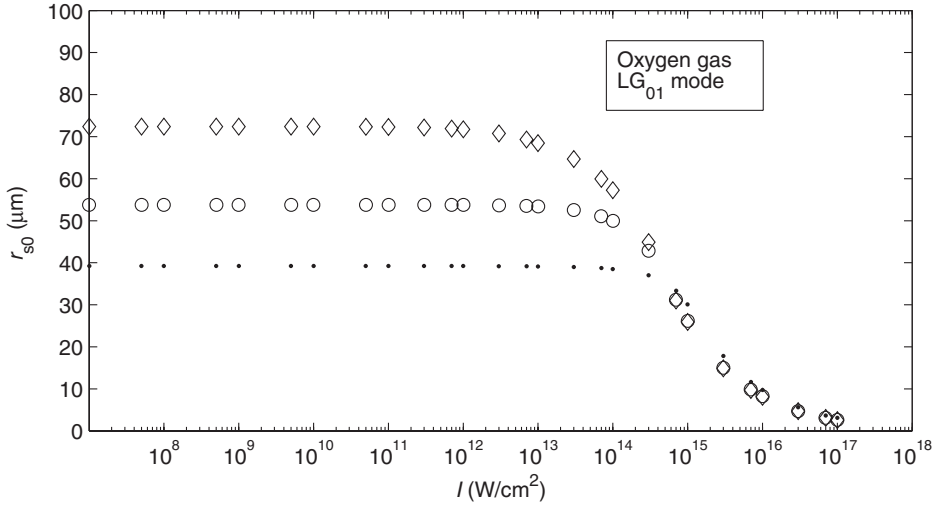


Figure 4. Variation of the matched initial spot sizes versus the intensity of the incident LG_{01} laser pulse propagating through a top-hat plasma channel with radius of $r_{ch} = 100\ \mu$m. Dot (·) for $\Delta n_{e,ch} = 1.67 \times 10^{18}\ cm^{-3}$, circle (○) for $\Delta n_{e,ch} = 1.67 \times 10^{17}\ cm^{-3}$ and diamond (◇) for $\Delta n_{e,ch} = 6.67 \times 10^{16}\ cm^{-3}$.

the relationship between the matched laser spot size and initial laser intensity for an arbitrary channel radius of $r_{ch} = 100\,\mu$m and different channel depth. It is seen that for $I \geqslant 1.2 \times 10^{14}\ W/cm^2$, the nonlinear Kerr effect becomes dominant and the optical guiding formulation does not hold. By increasing the intensity of the incident laser pulse, all solution branches of r_{s0} merge together and constitute a unique branch. The nonlinear Kerr effect shrink the guided laser radii to $r_{s0} < 10\,\mu$m at intensities $I > 10^{15}\ W/cm^2$. A similar behavior holds for LG_{01} mode. It is worth to note that further ionization by the propagating laser pulse does not change the optical guiding mechanism when $n_e'(r, z, \tau) < \Delta n_{e,ch}$. In this case, the main change is to increase the matched initial laser radius for a given channel radius. Change in electron density due to pondermotive force is not important, since the laser power is much less than the critical power for the pondermotive self-channeling.

4. Conclusions

In this paper we investigated the propagation of TEM_{00} and LG_{01} laser beams through a type of plasma channel that have top-hat refractive index. Assuming this profile for the plasma channel, the matched conditions for the laser beams were studied theoretically. It was found that the matched condition for the laser beams differ from the parabolic channel and hollow plasma waveguide. Unlike the parabolic channel, there are several solutions for matched laser initial spot size for the given values of channel depth and channel radius. At low intensities, where the nonlinear Kerr effect is negligible, there are minimum values for channel depth and channel radius in which the laser beam can be guided optically through the plasma channel. In order to account for the nonlinear Kerr effect, the matched condition were considered, too. It was found that the matched condition will be changed

https://doi.org/10.1017/S0022377811000341 Published online by Cambridge University Press

and the propagation characteristics changes drastically for high laser intensities. Our examinations of the top-hat plasma channel gave the impression that the refraction index profile of the capillary discharge at the early stage of the plasma formation is very important to guide the laser beam with a given spot size. Measured temporal variations of the laser pulse energy transmission through a capillary discharge [12, 13] indicate that the channel depth and the electron density profile (refractive index profile) are very important for guiding the laser pulse. Regarding this effect and our numerical results, one can optimize the transmission of laser pulse energy by adjusting not only by delay time between the laser pulse injection and onset of the discharge current pulse but also by laser pulse spot size.

Appendix A. Matched condition for a LG_{01} laser mode propagating in a top-hat plasma channel

Assuming the plasma channel with top-hat refractive index profile, a matched condition for the Laguerre–Gaussian laser beam with LG_{01} mode propagating through the plasma channel is derived by starting the wave equation for the laser electric field $\vec{E}(\vec{r},t)$ given by (2). In order to proceed the matched condition for the Laguerre–Gaussian laser pulse with LG_{01} mode, the following trail solution is assumed:

$$A(r,\theta,z,\tau)=B(z,\tau)\left[\sqrt{2}\frac{r}{r_s(z,\tau)}\right]e^{i\theta}e^{i\Phi(z,\tau)}e^{-[1-i\alpha(z,\tau)]\frac{r^2}{r_s^2(z,\tau)}}, \tag{A 1}$$

proceeding exactly in the same fashion as in Sec. 2, a set of self-consistent coupled equations for the pulse amplitude $B(z,\tau)$, phase $\Phi(z,\tau)$, wavefront curvature $\alpha(z,\tau)$ and spot size $r_s(z,\tau)$ can be derived. These coupled equations are

$$\frac{\partial B}{\partial z}=-\frac{2\alpha B}{kr_s^2}+F_I^{\mathrm{LG}}+G_I^{\mathrm{LG}}, \tag{A 2}$$

$$\frac{\partial \Phi}{\partial z}=-\frac{4}{kr_s^2}-2\frac{F_R^{\mathrm{LG}}}{B}-\frac{G_R^{\mathrm{LG}}}{B}, \tag{A 3}$$

$$\frac{\partial r_s}{\partial z}=\frac{2\alpha}{kr_s}-r_s\frac{G_I^{\mathrm{LG}}}{B}, \tag{A 4}$$

$$\frac{\partial \alpha}{\partial z}=\frac{2(1+\alpha^2)}{kr_s^2}+2\frac{G_R^{\mathrm{LG}}}{B}-2\alpha\frac{G_I^{\mathrm{LG}}}{B}. \tag{A 5}$$

The complex functions F^{LG} and G^{LG} used in (A.2)–(A.5) are given by

$$F^{\mathrm{LG}}=\frac{1}{4\pi k}\int_0^{2\pi}d\theta\int_0^{\infty}d\left(2\frac{r^2}{r_s^2}\right)S(r,\theta,z,\tau)\left(\sqrt{2}\frac{r}{r_s}\right)\times e^{-(1+i\alpha)\frac{r^2}{r_s^2}}e^{-i\Phi}e^{-i\theta}, \tag{A 6}$$

$$G^{\mathrm{LG}}=\frac{1}{8\pi k}\int_0^{2\pi}d\theta\int_0^{\infty}d\left(2\frac{r^2}{r_s^2}\right)S(r,\theta,z,\tau)\left(\sqrt{2}\frac{r}{r_s}\right)\times\left(2-2\frac{r^2}{r_s^2}\right)e^{-(1+i\alpha)\frac{r^2}{r_s^2}}e^{-i\Phi}e^{-i\theta}. \tag{A 7}$$

Substituting (5) into (A.6) and (A.7) yields

$$F^{\mathrm{LG}}(z,\tau)=-\frac{2}{kr_{s0}^2}B-\frac{\omega^2 n_2}{32k\pi c}|B|^2B+\frac{2\pi e^2 n_{e0}}{mc\omega}Be^N\times\left[\frac{N!}{(N+1)^{N+1}}\right]+\frac{2\pi e^2\Delta n_e B}{kmc^2}\left(\frac{r_s}{\sqrt{2}r_{ch}}\right)^{2N}\times\left[\frac{(N+1)!}{\left(N(\frac{r_s}{\sqrt{2}r_{ch}}\right)^2+1)^{(N+2)}}\right], \tag{A 8}$$

$$G^{\mathrm{LG}}(z,\tau)=-\frac{\omega^2 n_2}{128k\pi c}|B|^2B+\frac{\pi e^2 n_{e0}}{mc\omega}Be^N\left[\frac{N(N+1)!}{(N+1)^{N+3}}\right]+\frac{2\pi e^2\Delta n_e B}{kmc^2}\left(\frac{r_s}{\sqrt{2}r_{\mathrm{ch}}}\right)^{2N}\left[\frac{(N+1)!}{(N(\frac{r_s}{\sqrt{2}r_{\mathrm{ch}}})^2+1)^{(N+2)}}-\frac{(N+2)!/2}{\left(N(\frac{r_s}{\sqrt{2}r_{\mathrm{ch}}}\right)^2+1)^{N+3}}\right]. \tag{A 9}$$

The matched condition leads to an equation with order of $2N+8$ given by

$$b_1x^{2N+2}\left[(N+1)!\frac{N}{2}(1-2x^2)\right]-\left[1-b_4|B|^2x^2+b_5n_{e0}e^Nx^2\right](Nx^2+1)^{N+3}=0, \tag{A 10}$$

where $b_4=b_2/4$ and $b_5=2\pi r_e r_{\mathrm{ch}}^2[N(N+1)!/(N+1)^{N+3}]$. This equation for given values of b_1, $b_4|B|^2$ and $b_5n_{e0}e^N$ gives real and positive roots for matched guiding.

References

[1] Milchberg, H. M., Durfee, C. G. and Lynch, J. 1995 *J. Opt. Soc. Am.* B **12**, 731.

[2] Janulewicz, K. A., Rocca, J. J., Bortolotto, F., Kalachnikov, M. P., Shlyaptsev, V. N., Sandner, W. and Nickles, P. V. 2001 *Phys. Rev.* A **63**, 03 3803.

[3] Korobkin, D., Nam, C. H., Suckewer. S. and Goltsov, A. 1996 *Phys. Rev. Lett.* **77**, 5206.

[4] Butler, A., Gonsalves, A. J., McKenna, C. M., Spence, D. J., Hooker, S. M., Sebban, S., Mocek, T., Bettaibi, I. and Cros, B. 2003 *Phys. Rev.* A **91**, 20 5001.

[5] Tajima, T. and Dawson, J. M. 1979 *Phys. Rev. Lett.* **43**, 267.

[6] Sprangle, P., Esarey, E., Ting, A. and Joyce, G. 1988 *Appl. Phys. Lett.* **53**, 2146.

https://doi.org/10.1017/S0022377811000341 Published online by Cambridge University Press

[7] Borisov, A. B., Borovskii, A. V., Korobkin, V. V., Prokhorov, A. M., Shiriaev, O. B., Shi, X. M., Luk, T. S., McPherson, A., Solem, J. C. and Boyer, 1992 *K. Phys. Rev. Lett.* **68**, 2309.

[8] Clayton, C. E., Tzeng, K. C., Gordon, D., Muggli, P., Mori, W. B., Joshi, C., Malka, V., Najmudin, Z., Modena, A., Neely, D., et al. 1998 *Phys. Rev. Lett.* **81**, 100.

[9] Hosokai, T., Kando, M., Dewa, H., Kotaki, H., Kondo, S., Nakajima, K. and Horioka, K. 2000 *Opt. Lett.* **25**, 10.

[10] Jackel, S., Burris, R., Grun, J., Ting, A., Manka, C., Evans, K. and Kosakowskii, J. 1995 *Opt. Lett.* **20**, 1086.

[11] Courtois, C., Cros, B., Malka, G., Matthieussent, G., Marquès, J. R., Blanchot, N. and Miquel, J. L. 2000 *J. Opt. Soc. Am.* B: *Opt. Phys.* **17**, 864.

[12] Luther, B. M., Wang, Y., Marconi, M. C., Chilla, J. L. A., Larotonda, M. A. and Rocca, J. J. 2004 *Phys. Rev. Lett.* **92** , 23 5002.

[13] Spence, D. J. and Hooker, S. M. 2000 *Phys. Rev.* E **63**, 01 5401; Butler, A., Spence, D. J. and Hooker, S. M. 2002 *Phys. Rev. Lett.* **89**, 18 5003; Spence, D. J., Butler, A. and Hooker, S. M. 2001 *J. Phys.* B: *At. Mol. Opt. Phys.* **34**, 4103.

[14] Durfee, C. G. and Milchberg, H. M. 1993 *Phys. Rev. Lett.* **71**, 2409.

[15] Malka, V., De Wispelaere, E., Amiranoff, F., Baton, S., Bonadio, R., Coulaud, C. and Haroutunian, R. 1997 *Phys. Rev. Lett.* **79**, 2979.

[16] Faure, J., Malka, V., Marques, J. R., Amiranoff, F., Courtois, C., Najmudin, Z., Krushelnick, K., Salvati, M., Dangor, A. E., Solodov, A., et al. 2000 *Phys. Plasmas* **7**, 3009.

[17] Nikitin, S. P., Antonsen, T. M., Clark, T. R., Yuelin, L. and Milchberg, H. M. 1997 *Opt. Lett.* **22**, 1787.

[18] Gaul, E. W., Le Blanc, S. P., Rundquist, A. R., Zgadzaj, R., Langhoff, H. and Downer, M. C. 2000 *Appl. Phys. Lett.* **77**, 4112.

[19] Volfbeyn, P., Esarey, E. and Leemans, W. P. 1999 *Phys. Plasmas* **6**, 2269.

[20] Leemans, W. P., Nagler, B., Gonsalves, A. J., Toth, Cs., Nakamura, K., Geddes, C. G. R., Esarey, E., Schroeder, C. B. and Hooker, S. M. 2006 *Nature Phys.* **2**, 696.

[21] Leemans, W. P., Volfbeyn, P., Guo, K. Z., Chattopadhyay, S., Schroeder, C. B., Shadwick, B. A., Lee, P. B., Wurtele, J. S. and Esarey, E. 1998 *Phys. Plasmas* **5**, 1615.

[22] Esarey, E. and Leemans, W. P. 1999 *Phys. Rev.* E **59**, 1082.

[23] Sprangle, P., Hafizi, B. and Peñano, J. R. 2000 *Phys. Rev.* E **61**, 4381.

[24] Chen, G. L., Lu, H. Y., Wang, C., Liu, J. S., Li, R. X., Nia, G. Q. and Xu, Z. Z. 2008 *Eur. Phys. J.* D **47**, 303.

[25] Chiou, T. C., Katsouleas, T., Decker, C., Mori, W. B., Wurtele, J. S., Shvets, G. and Su, J. J. 1995 *Phys. Plasmas* **2**, 310.

[26] Couairon, A., Tzortzakis, S., Berge, L., Franco, M., Prade, B. and Mysyrowicz, A. 2002 *J. Opt. Soc. Am.* B **19**, 1117.

[27] Sprangle, P., Ting, A. and Tang, C. M. 1897 *Phys. Rev.* A **36**, 2773.

https://doi.org/10.1017/S0022377811000341 Published online by Cambridge University Press